Journal of Materials Science: Materials in Electronics (2019) 30:8007–8013
https://doi.org/10.1007/s10854-019-01121-6

# Investigating the electrical characteristics of a single electron transistor utilizing graphene nanoribbon as the island

Vahideh Khademhosseini[1] · Daryoosh Dideban[1,2] · MohammadTaghi Ahmadi[3,4] · Razali Ismail[4] · Hadi Heidari[5]

Received: 4 November 2018 / Accepted: 11 March 2019 / Published online: 19 March 2019


**Abstract**
Single electron transistor (SET) is a fast device with promising features in nanotechnology. Its operation speed depends on the island material, so a carbon based material such as graphene nanoribbon (GNR) can be a suitable candidate for using in SET island. The GNR band gap which depends on its width, has a direct impact on the coulomb blockade and SET current. In this research, current–voltage characteristic for the SET utilizing GNR in its island is modelled. The comparison study shows the impact of GNR width and length on the SET current. Furthermore SET quantum capacitance is modeled and effect of GNR width and temperature on the quantum capacitance are investigated.

## 1 Introduction

Tunneling based devices such as single electron transistor (SET) are attractive subjects for researchers. This nanoscale transistor has promising features such as very fast switching speed and its operation is based on quantum tunneling [1, 2]. A single electron tunnels from source electrode to the island and then leaves it to drain electrode [3, 4]. This process is prevented by coulomb blockade phenomena. It affects on the energy levels of the island as well as source and drain electrodes [5, 6]. If energy level of the electron in the island is between energy levels of drain and source (transfer window), the electron can tunnel and current flows [7]. The island shape and its material properties such as electron mobility have direct effect on the SET current and Coulomb Blockade (CB) range [8]. On the other hand theoretical and experimental works on SETs utilizing 2D materials have been researched and reported in [9–11]. SET material can be graphene which is 2D structure of carbon atoms arranged in a hexagonal pattern [12]. The interesting characteristics of this 2D material is discovered by Geim and Novoselov from the University of Manchester at 2004 [13]. It has high carrier mobility, so graphene SET can operate with a high speed. A strip of graphene is called graphene nanoribbon (GNR) and it has one dimensional structure [14, 15]. Its edge configurations has two different types called armchair and zigzag [16–18]. The armchair configuration is classified to three families: 3p, 3p + 1 and 3p + 2 where "p" is an integer number indicating the number of atoms along the width [19]. The corresponding bandgaps with same "p"'s are different for each family, so the current which flows from graphene SET depends on the energy gap [19, 20]. In other words, GNR bandgap depends on its edge configuration and number of atoms along its width [21]. GNRs can be used in applications such as nanoribbon field effect transistors and other nanoscale devices. On the other hand, the SET operates based on the transfer of few and even one electron. Therefore it can be utilized in precise sensors. This device is very sensitive, so it can be used in detection of infrared and microwave radiations. Since the island material has a direct impact on the SET performance, using GNR with different widths as the island can tune the CB range of the SET and thus, the sensitivity or performance of the target device can be tuned. We derive the current–voltage characteristics for a SET utilizing graphene in this research and then study the impact of GNR width and length on the current.

✉ Vahideh Khademhosseini
v_khademhosseini@grad.kashanu.ac.ir

1 Institute of Nanoscience and Nanotechnology, University of Kashan, Kashan, Iran

2 Department of Electrical and Computer Engineering, University of Kashan, Kashan, Iran

3 Nano electronic Research Group, Physics Department, Nanotechnology Research Center, Urmia University, Urmia, Iran

4 Faculty of Electrical Engineering, Universiti Teknologi Malaysia, 81310 Johor Bahru, Johor, Malaysia

5 Microelectronics Lab, Electronics and Nanoscale Engineering Research Division, School of Engineering, University of Glasgow, Glasgow, UK

## 2 Modelling the current flow in a GNR SET

A single electron transistor comprises of source, gate, drain electrodes and an island which is located between source and drain but not connected to them as shown in Fig. 1a. The GNR island with the length of $L$ can be assumed as a quantum well and the potential profile along the device is shown in Fig. 1b. Schrodinger equation can be employed to derive the electron wave function and the corresponding current for this particular device.

The wave functions for different parts of SET (regions I, II, III) is given by:

$$\Psi_I = A_1 e^{k_1 x} + B_1\, e^{-k_1 x} \tag{1}$$

$$\Psi_{II} = A_2 e^{ik_2 x} + B_2\, e^{-ik_2 x} \tag{2}$$

$$\Psi_{III} = A_3 e^{ik_3 x} \tag{3}$$

where $k_1 = k_3 = \frac{\sqrt{2m(V_0 - E)}}{\hbar}$ and $k_2 = \frac{\sqrt{2mE}}{\hbar}$.

Continuity of the wave functions and its derivative for the neighbouring parts gives the boundary conditions at $x = 0$ and L as:

$$A_1 + B_1 = A_2 + B_2 \tag{4}$$

$$k_1 A_1 - k_1 B_1 = ik_2 A_2 - ik_2 B_2 \tag{5}$$

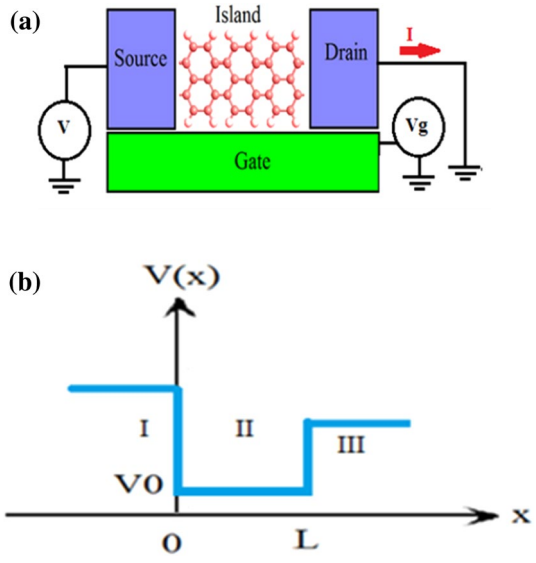


**Fig. 1** **a** Graphene nanoribbon SET with its biasing at different electrodes. **b** The potential profile along the device

$$A_2 e^{ik_2 L_1} + B_2 e^{-ik_2 L_1} = A_3 e^{k_1 L_1} \tag{6}$$

$$ik_2 A_2 e^{ik_2 L_1} - ik_2 B_2 e^{-ik_2 L_1} = k_1 A_3 e^{k_1 L_1} \tag{7}$$

Therefore the transmission coefficient of electrons in GNR SET can be calculated as [22]:

$$T = \frac{1}{1 + \frac{(\mathrm{h}^2 + ta'm)E - \hbar^2 E_g}{2\sqrt{ta`\mathrm{h}mE(E - E_g)}} sinh^2(k_2 L)} \tag{8}$$

where "$L$" is the GNR length, $k_2 = \frac{\sqrt{2mE}}{\hbar}$, "$E$" is the electron energy level, "$m$" is the electron effective mass, "$h$" is the Planck's constant, "$a' = 3a_{c-c}$", and $a_{c-c} = 1.42A^0$ sis the distance between neighbouring carbon atoms, "$E_g$" is the GNR band gap and "$t = 2.7$ eV". The current of GNR SET is modeled by using transmission coefficient and Landauer equation [22]. On the other hand the relation between bandgap and GNR width ($w$) for 3p + 1 family is [23, 24]:

$$E_g = \frac{1.04eV}{w(nm)} \tag{9}$$

Therefore current of GNR SET is modeled as:

$$I = \int_o^{\eta} \frac{AK_BTx\left(K_BTx + \frac{1.04}{w}\right)}{AK_BTx\left(K_BTx + \frac{1.04}{w}\right) + \left(B\left(K_BTx + \frac{1.04}{w}\right) + CAK_BTx\right)^2 \left[\left(B\left(K_BTx + \frac{1.04}{w}\right)L^2\right)^{\frac{1}{2}} + \frac{\left(B\left(K_BTx + \frac{1.04}{w}\right)L^2\right)^{\frac{3}{2}}}{6}\right]^2} \cdot \frac{dx}{e^{x-\eta} + 1} \tag{10}$$

where $A = \left(\frac{16m}{3\hbar ta_{c-c}}\right)$, $B = \left(\frac{2m}{\hbar}\right)$, $C = \left(\frac{2}{3ta_{c-c}}\right)$, $x = \frac{E - E_g}{K_BT}$, $\eta = \frac{E_F - E_g}{K_BT}$, "$E_F$" is GNR Fermi energy, "$K_B$" is Boltzmann's constant, and other parameters were defined previously. It is worth noting that the GNR width is directly proportional to the number of carbon atoms along the ribbon width. In general, the relation between the width and the number carbon atoms in an armchair GNR is given by [23, 24]:

$$w(nm) = \frac{0.246}{2}(N - 1) \tag{11}$$

Figure 2 represents an armchair GNR having 7 carbon atoms along the width. Since the current in Eq. (10) is explicitly based on the GNR width, the SET current can be evaluated for different ribbon widths as shown in Fig. 3. This figure reveals the fact that the highest GNR width has the lowest coulomb blockade (CB) range and zero current. In the other words, increasing GNR width increases the probability of electron tunneling and this leads to increase in the current. Figure 4 indicates current versus the gate voltage for the proposed device. This is in agreement with the fluctuating behavior of the current in SET devices.

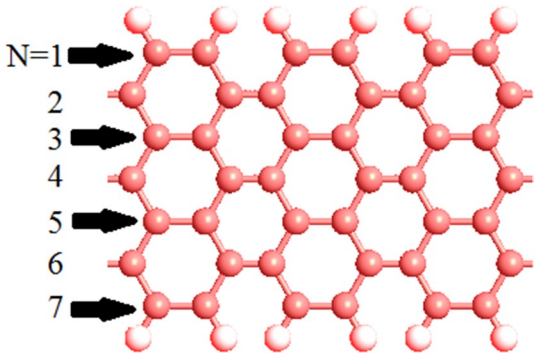


**Fig. 2** An armchair GNR with N = 7

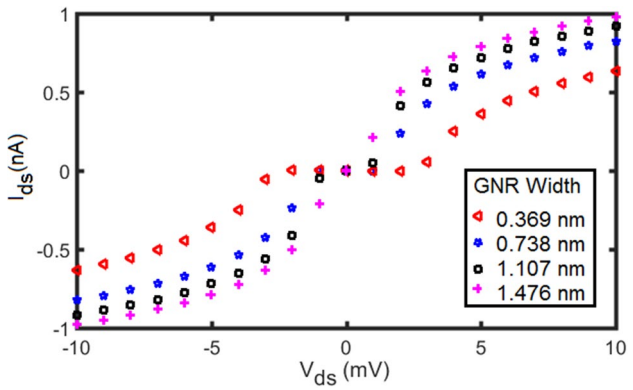


**Fig. 3** SET current ($I_{ds}$) versus drain-source voltage ($V_{ds}$) for different island widths, gate voltage is 1 mV and GNR length is 0.492 nm

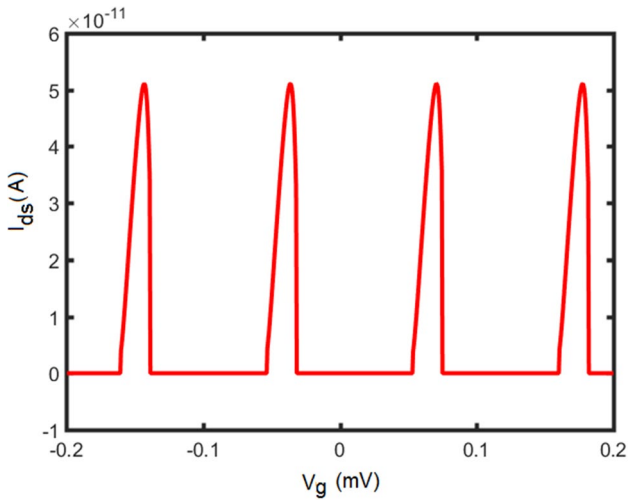


**Fig. 4** SET current ($I_{ds}$) versus gate voltage ($V_g$) characteristic in GNR SET

SET current versus the drain voltage is plotted in Fig. 5 while the GNR length and width are selected as 0.369 nm and 0.492 nm, respectively. This figure clearly shows that

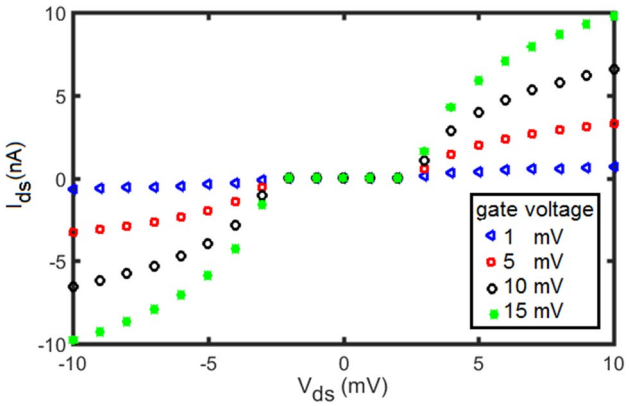


**Fig. 5** SET current ($I_{ds}$) versus drain-source voltage ($V_{ds}$) for different gate voltages. GNR width and length are 0.369 nm and 0.492 nm, respectively

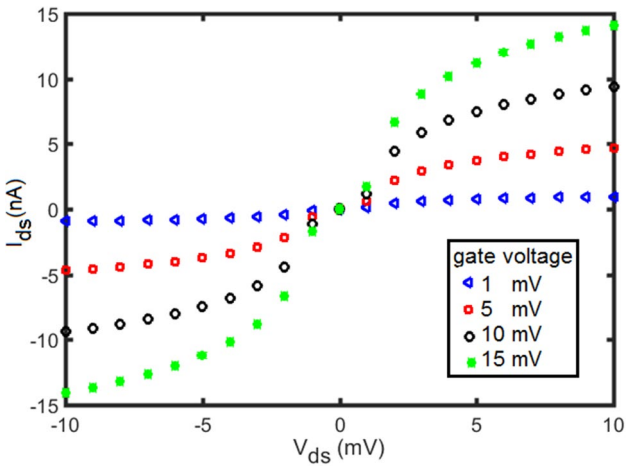


**Fig. 6** SET current ($I_{ds}$) versus drain-source voltage ($V_{ds}$) for different gate voltages. GNR width and length are 1.23 nm and 0.492 nm, respectively

increasing of the gate voltage has no significant impact on the coulomb blockade (CB) range. However, the gate voltage has a direct impact on the SET current for the $V_{ds}$ outside from CB range. In order to evaluate the impact of gate voltage on the current, we simulated another device with the GNR width of 1.23 nm as shown in Fig. 6. Comparison of Figs. 5 and 6 indicates that the current in the device having wider GNR is almost 1.5 times more than the corresponding current of the other device. Furthermore, CB range is about one nanovolt for the device utilizing wider GNR but it is several millivolts for the device with smaller GNR width. Coulomb blockade (CB) is a limitation in the operation of SET devices because it presents a region where the current is zero. For wider nanoribbons, the CB range is lower than narrow ones because its bandgap values is lower in wider nanoribbon as shown in

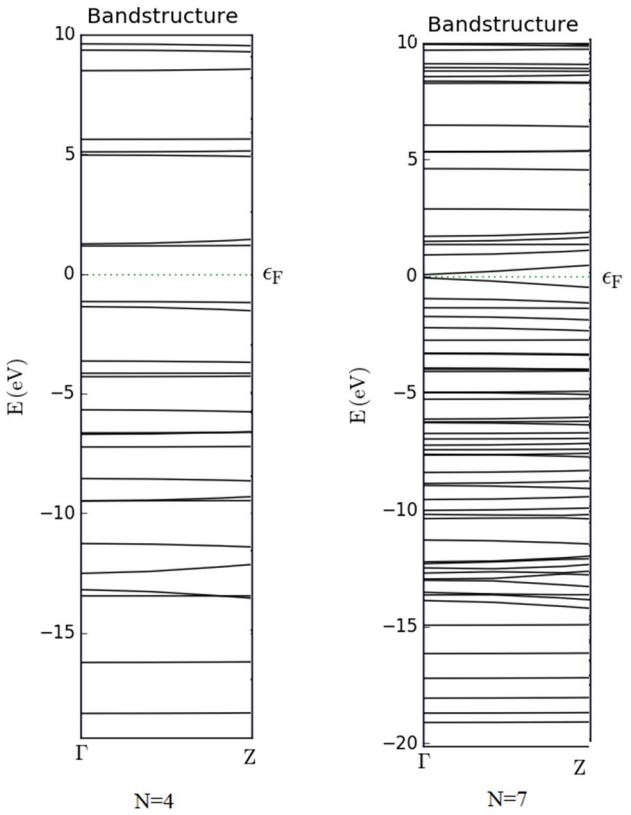


**Fig. 7** The band structures of the graphene nanoribbon with different carbon atoms in GNR width. **a** Four carbon atoms in GNR width **b** seven carbon atoms in GNR width

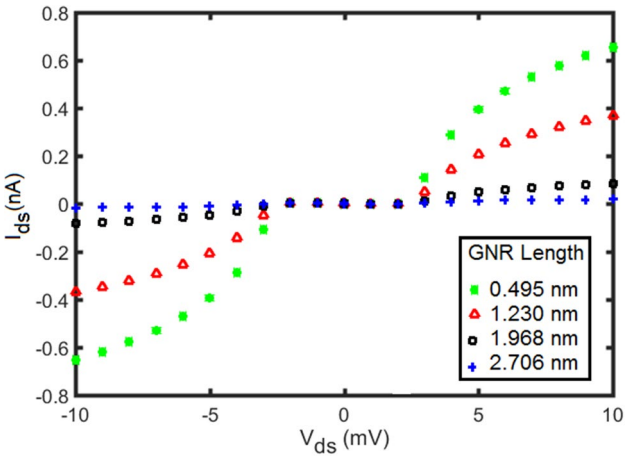


**Fig. 8** SET current ($I_{ds}$) versus drain-source voltage ($V_{ds}$) for different GNR lengths. Gate voltage is 1 mV and GNR width is 0.369 nm

Fig. 7. It can be seen that the bandgap value for GNR with the width of 7 carbon atoms is 0.124 eV while it is much higher (2.3 eV) for the GNR with just 4 atoms across the width. Therefore with increase in the GNR width, electron transfer speed increases and zero current range and consequently CB range decreases.

The impact of GNR length on the SET current is investigated and shown in Fig. 8. It clearly indicates that variation in the GNR length, like the gate voltage, has no significant impact on the CB range. On the other hand, GNR length has a direct impact on the device current for the.

$V_{ds}$ outside from CB range. The physical reason behind this behavior is that increasing the GNR length leads to a longer potential barrier in the island. This leads to decreased tunneling of electrons from source to drain and thus, the SET current is significantly reduced.

## 3 Investigating the quantum capacitance and charge stability diagram

Quantum capacitance ($C_Q$) is an important parameter for low dimensional materials. The quantum capacitance of $MoS_2$ and bilayer graphene are calculated by other researchers [25, 26]. $C_Q$ of bilayer graphene is based on the band structure and density of states which is then expressed as function of energy and energy broadening parameter (Γ) [25]. The band-edge density of states (*DOS*) is a function of spin and valley degeneracy factors. The intrinsic carrier density is modeled based on the bandgap energy and the local channel electrostatic potential. Lastly, the quantum capacitance is modeled as function of temperature [26].

In this research GNR is selected for SET island. GNR is carbon based material with high electron mobility and high speed of transfer electron. Although SET has a very fast switching speed but island material has a direct impact on the operation speed. Graphene is a low dimensional material and thus, its quantum capacitance ($C_Q$) is located in series with geometrical capacitance ($C_{GEO}$) of the SET tunnel junctions. On the other hand quantum capacitance has smaller value compared with geometrical capacitance, so it degrades the total capacitance based on the following equation:

$$\frac{1}{C_{total}} = \frac{1}{C_Q} + \frac{1}{C_{GEO}} \tag{12}$$

The quantum capacitance is an important component in very small dimension electronic devices. It is comprehensively modeled in our previous research [27]. Here we briefly derive the equations need for its derivation and then investigate the impact of GNR width and temperature on its behavior:

$$C_Q = \frac{\partial Q}{\partial V_g} = e^2 \frac{\partial n}{\partial E} \tag{13}$$

where "$e$" is electron charge, "$n$" is the carrier density and "$E$" is the carrier energy. The carrier density can be calculated from:

$$n = \int DOS(E).f(E)dE \tag{14}$$

where "$f(E)$" is the Fermi distribution function and "$DOS(E)$" denotes the density of states at a given energy which is given by [27]:

$$DOS(E) = \frac{(ta''')^{\frac{-1}{2}}}{2\sqrt{2\pi}}(eV_g - E_0)^{\frac{-1}{2}} \tag{15}$$

where "$V_g$" is the gate voltage, "$E_0$" is the band gap of GNR, "$t = 2.7eV$" is the nearest neighbor C–C tight-binding overlap energy,"$a''' = 3a_{c-c}$" and $a_{c-c} = 1.42A°$ is the carbon–carbon bond length. Substitution of Eq. 15 into Eq. 14, gives the carrier density:

$$n = \frac{(ta''')^{\frac{-1}{2}}}{2\sqrt{2}\pi}\int_0^{\infty}\frac{(E-E_0)^{\frac{-1}{2}}}{\exp(\frac{(E-E_F)}{k_BT}+1}dE \tag{16}$$

Finally, substituting Eq. 16 into Eq. 13 gives the quantum capacitance:

$$C_Q = e^2\frac{\partial n}{\partial E} = e^2\frac{(ta''')^{\frac{-1}{2}}}{2\sqrt{2\pi}}.\frac{(E-E_0)^{\frac{-1}{2}}}{\exp(\frac{(E-E_F)}{k_BT}+1} \tag{17}$$

It is worth noting that since $E = e.V_g$, Eq. 17 can be evaluated to investigate the impact of gate voltage ($V_g$) and temperature ($T$) on the quantum capacitance or the carrier density. This is due to the fact that variation of the carrier density with respect to $V_g$ is the same as $C_Q$ but scaled by the charge on an electron:

$$C_Q = e\frac{\partial n}{\partial V_g} \text{ or} \frac{\partial n}{\partial V_g} = \frac{C_Q}{e} \tag{18}$$

The carrier mobility is calculated for the GNR island of SET as [25]:

$$\mu_{SET} = \frac{dI}{dV_g}(\frac{L}{W})\frac{1}{V_{ds}}\frac{C_{GEO}+C_Q}{C_{GEO}C_Q} \tag{19}$$

where "$I$" is SET current, "$V_g$" is the gate voltage, "$L$" is GNR length, "$W$" is GNR width, "$V_{ds}$" is drain- source voltage, "$C_{GEO}$" is geometric capacitance and "$C_Q$" is the quantum capacitance.

Furthermore its variation with gate voltage at room temperature can be calculated as:

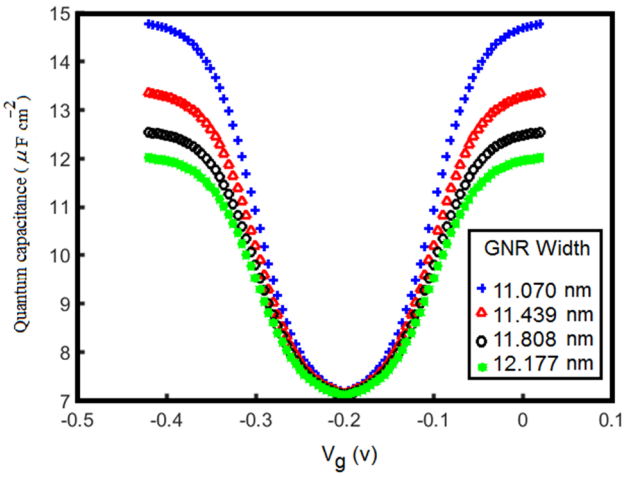


**Fig. 9** Quantum capacitance versus gate voltage ($V_g$) for different GNR widths

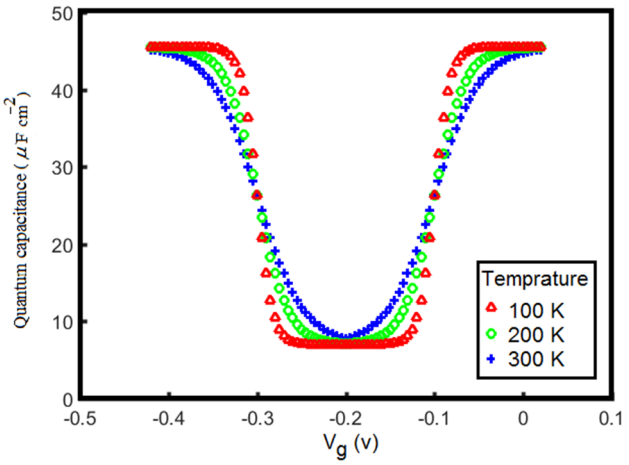


**Fig. 10** Quantum capacitance versus gate voltage ($V_g$) at different temperatures where GNR width is 11.07 nm

$$\frac{d\mu_{SET}}{dV_g} = \frac{d^2I}{d^2V_g}(\frac{L}{w})\frac{1}{V_{ds}}\frac{C_{GEO}+C_Q}{C_{GEO}C_Q} \tag{20}$$

In this research, we investigate the impact of GNR width and temperature on the quantum capacitance. The proposed model is explicitly based on GNR width, and the effect of this parameter on the quantum capacitance is illustrated in Fig. 9. Analysis of Fig. 9 indicates that increasing GNR width decreases the maximum value of the quantum capacitance while its impact on the minimum value (which occurs around $V_g = -0.2V$) is not noticeable. This minimum value is arbitrary that depends on the reference electrode.

The impact of temperature on the quantum capacitance is depicted Fig. 10. It reveals the fact that the temperature

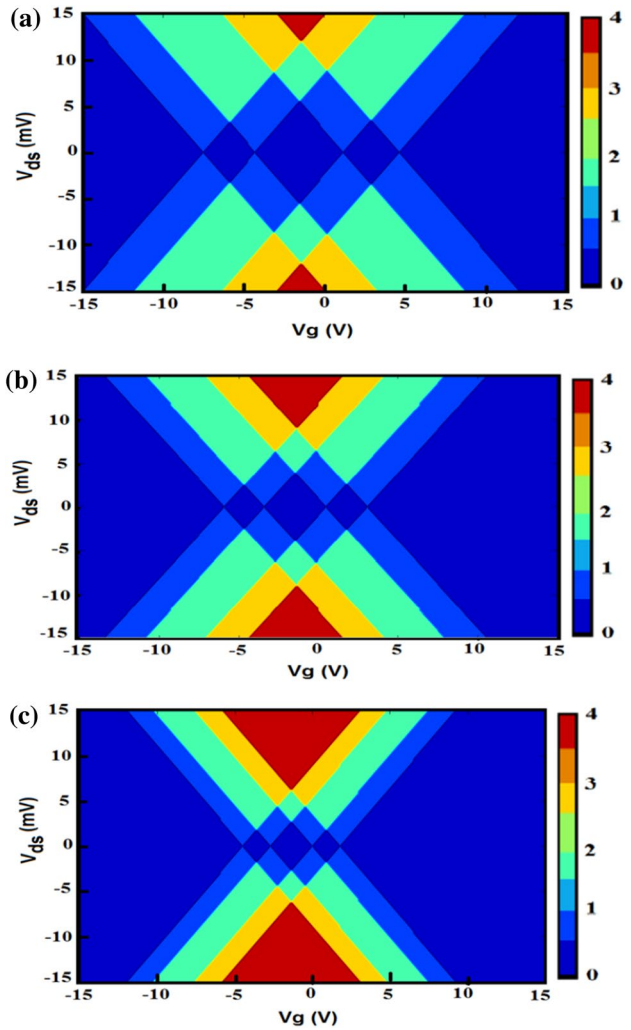


**Fig. 11** The simulated charge stability diagrams for three GNR SETs with different number of atoms along the width (the color bar on the right side of each figure represents the corresponding charge states in the diagram),: **a** GNR island with N = 4, **b** GNR island with N = 7, **c** GNR island with N = 10

in neither influence on the maximum nor minimum value of the quantum capacitance. Instead, the quantum capacitance is broadened at higher temperatures. This behavior is due to the fact that the Fermi function is broadened at higher temperatures. It is worth noting that the minimum quantum capacitance for both Figs. 9 and 10 happens around − 0.2 V. This is due to the fact that based on Eq. (13), the minimum occurs at $E = eV_g = E_F$ where *"e"* is the unit charge and *"$E_F$"* is the GNR fermi energy. In order to calibrate the simulated quantum capacitance against real measured data presented in [28], $E_F$ is selected such that this minimum appears around − 0.2V.

The GNR SETs with different GNR widths are designed and simulated with Atomistic Toolkit software [29]. GNRs with 4, 7 and 10 carbon atoms along their widths in *xyz* coordinates are simulated with Atomistix ToolKit (ATK)* software. The DFT method using local-density approximation (LDA) is selected for simulations. The simulation result reveals the highest occupied molecular orbital (HOMO) and lowest unoccupied molecular orbital (LUMO) levels. Their charge stability diagrams are plotted in Fig. 11a–c corresponding to 4, 7 and 10 carbon atoms along the GNR width, respectively. The blue diamonds in each figure presents regions where the tunneling is completely stopped due to coulomb blockade effect and thus, no current is flowing through the device.

Based on the charge stability diagrams shown in Fig. 11 for different GNR widths, it is concluded that increasing the number of carbon atoms along GNR width decreases the coulomb diamond area and CB range. This result is in agreement with what we found from Fig. 3. With comparison of the charge stability diagram in Fig. 11a with $I_d$–$V_{ds}$ characteristics shown in Fig. 5, as both figures represent the behavior of a GNR SET with the same length and width, it is concluded that they both give a CB range between − 3 to 3 mV at very small gate voltages and the results are consistent together.

It is worth noting that The GNR in SET environment shows lower charging energy than GNR in the non-SET environment because charge is stable on GNR molecule by the electrostatic surrounding. On the other hand, the coulomb blockade (CB) phenomenon is a unique property of SET and cannot be seen on non-SET environment. In addition to that, with utilizing GNR in the island part of SET and taking some of its advantages including its high mobility and bandgap control, a very fast and tunable device can be obtained simultaneously.

## 4 Conclusion

In this research, a single electron transistor utilizing graphene nanoribbon as the island was investigated. The emphasis was to model the current behavior versus ribbon geometry (width and length) and the gate voltage. The results revealed the fact that increasing GNR width leads to decrease of the coulomb blockade (CB) range. However, the GNR length and gate voltage did not have a noticeable impact on the CB range but these parameters showed a significant impact on the SET current for the drain voltages outside from CB range. Moreover quantum capacitance was modeled and the effects of GNR width and temperature was investigated. The charge stability diagrams were simulated and the results showed that increasing the number of carbon atoms along the GNR width has a direct effect on CB range and coulomb diamond area.

**Acknowledgements** This research was supported by University of Kashan under supervision of Dr. Daryoosh Dideban. Authors are thankful to the support received for this work from Micoelectronics Lab (meLab) at the University of Glasgow, UK. Also thanks to the Research Management Center (RMC) of Universiti Teknologi Malaysia (UTM) for providing an excellent research environment in which to simulate this research by Atomistix ToolKit and to complete this work.

## References

1. H. Park, J. Park, A.K.L. Lim, E.H. Anderson, A.P. Alivisatos, P.L. McEuen, Nano mechanical oscillations in a single-C60 transistor. Nature **407**, 57–60 (2000)
2. V. KhademHosseini, D. Dideban, M.T. Ahmadi, R. Ismail, An analytical approach to model capacitance and resistance of capped carbon nanotube single electron transistor. Int. J. Electron. Commun. (AEÜ) **90**, 97–102 (2018)
3. J. Park, A.N. Pasupathy, J.I. Goldsmith, C. Chang, Y. Yaish, J.R. Rinkoski, J.P. Sethna, H.D. Abruña, P.L. McEuen, D.C. Ralph, Coulomb blockade and the Kondo effect in single-atom transistors. Nature **417**, 722–725 (2002)
4. V. KhademHosseini, D. Dideban, M.T. Ahmadi, R. Ismail, Analysis of co-tunneling current in fullerene single-electron transistor. Braz. J. Phys. **48**(4), 406–410 (2018)
5. H. Zheng, M. Asbahi, S. Mukherjee, C.J. Mathai, K. Gangopadhyay, J.K.W. Yang, S. Gangopadhyay, Room temperature Coulomb blockade effects in Au nanocluster/pentacene single electron transistors. Nanotechnology. **26**, 355204 (2015)
6. V.K. Hosseini, M.T. Ahmadi, S. Afrang, R. Ismail, Analysis and simulation of coulomb blockade and coulomb diamonds in fullerene single electron transistors. Nano Electron. Optoelectron. **13**, 138–143 (2018)
7. V.K. Hosseini, M.T. Ahmadi, S. Afrang, R. Ismail, Analysis of Coulomb blockade in fullerene single electron transistor at room temperature. J. Nanoanal. **4**(2), 120–125 (2017)
8. V. KhademHosseini, M.T. Ahmadi, R. Ismail, Analysis and modeling of fullerene single electron transistor based on quantum dot arrays at room temperature. J. Electron. Mater. **47**(8), 4799–4806 (2018)
9. C. Stampfer, E. Schurtenberger, F. Molitor, J. Güttinger, T. Ihn, K. Ensslin, Tunable graphene single electron transistor. Nano Lett. **8**(8), 2378–2383 (2008)
10. S.J. Ray, First-principles study of $MoS_2$, phosphorene and graphene based single electron transistor for gas sensing applications, Sens. Actuator B **222**, 492–498 (2016)
11. S.J. Ray, M.V. Kamalakar, R. Chowdhury, Ab initio studies of phosphorene island single electron transistor. J. Phys. **28**(19), 195302 (2016)
12. K.S. Novoselov, A.K. Geim, S. Morozov, Two dimensional gas of massless Dirac fermions in graphene. Nature **438**(7065), 197–200 (2005)
13. K.S. Novoselov, A.K. Geim, S.V. Morozov, Electric field in atomically thin carbon films. Science **306**(5696), 666–669 (2004)
14. J.P. Llinas, A. Fairbrother, G.B. Barin, W. Shi, K. Lee, S. Wu, B.Y. Choi, R. Braganza, J. Lear, N. Kau, W. Choi, C. Chen, Z. Pedramrazi, T. Dumslaff, A. Narita, X. Feng, K.M.F. Fischer, A. Zettl, P. Ruffieux, E. Yablonovitch, M. Crommie, R. Fasel, J. Bokor, Short-channel field-effect transistors with 9-atom and 13-atom wide graphene nanoribbons. Nat. Commun. **8**(633), (2017)
15. J. Fang, S. Chen, W.G. Vandenberghe, M.V. Fischetti, Theoretical study of ballistic transport in silicon nanowire and graphene nanoribbon field-effect transistors using empirical pseudopotentials. IEEE Trans. Electron Devices **64**(6), 2758–2764 (2017)
16. D. Li, D. Wu, X. Zhang, B. Zeng, M. Li, H. Duan, B. Yang, M. Long, The spin-dependent electronic transport properties of $M(dcdmp)_2$ (M = Cu, Au, Co, Ni) molecular devices based on zigzag graphene nanoribbon electrodes. Phys. Lett. A **382**(21), 1401–1408 (2018)
17. J. Hur, D. Kim, Theoretical investigation of performance of armchair graphene nanoribbon field effect transistors. Nanotechnology 29(18), 185202 (2018)
18. G. Li, K.Y. Yoon, X. Zhong, J. Wang, R. Zhang, J.R. Guest, J. Wen, X.Y. Zhu, G. Dong, A modular synthetic approach for band-gap engineering of armchair graphene nanoribbons. Nature Commun. **9**, 1687 (2018)
19. W. Wang, M. Zhou, X. Li, S. Li, X. Wu, W. Duan, L. He, Energy gaps of atomically precise armchair graphene sidewall nanoribbons. Phys. Rev. B **93**, 241403 (2016)
20. Y.W. Son, M.L. Cohen, S.G. Louie, Half-metallic graphene nanoribbons. Nature **444**, 347–349 (2006)
21. N. Merino-Díez, A.G. Lekue, E.C. Sanromà, J. Li, M. Corso, L. Colazzo, F. Sedona, D.S. Portal, J.I. Pascual, D.G. de Oteyza, Width-dependent band gap in armchair graphene nanoribbons reveals fermi level pinning on Au(111). ACS Nano, **11**(11), 11661–11668 (2017)
22. V. Khademhosseini, M.T. Ahmadi, S. Afrang, R. Ismail, Current analysis and modelling on fullerene single electron transistor at room temperature. J. Electron. Mater. **46**(7), 4294–4298 (2017)
23. C.N. Bondja, Z. Geng, R. Granzner, J. Pezoldt, F. Schwierz, Simulation of 50-nm gate graphene nanoribbon transistors. Electronics, **5**(3), 1–17 (2016)
24. H. Raza, E.C. Kan, Armchair graphene nanoribbons: electronic structure and electric-field modulation, Phys. Rev. B **77**, 245434 (2008)
25. N. Ma, D. Jena, Carrier statistics and quantum capacitance effects on mobility extraction in two-dimensional crystal semiconductor field-effect transistors. 2D Mater. **2**, 015003 (2015)
26. G.S. Kliros, A Phenomenological model for the quantum capacitance of monolayer and bilayer graphene devices. Rom. J. Inf. Sci. Technol. 11 (2011)
27. V.K. Hosseini, D. Dideban, M.T. Ahmadi, R. Ismail, Analysis and modelling of quantum capacitance on graphene single electron transistor. Int. J. Mod. Phys. B **32**(22), 1850235 (2018)
28. J. Xia, F. Chen, J. Li, N. Tao, Measurement of the quantum capacitance of graphene. Nat. Nanotechnol. **4**, 505 (2009)
29. https://quantumwise.com/products/atk. Accessed Nov 2018